A Thesis

On

Investigations on Diffuse Reflectance of Aluminium Doped Titania

Submitted in the partial fulfilment of requirement for the award of the

Degree of

Master of Science (PHYSICS)

Submitted by: Meenu

Roll No.: 300804015

Under the Guidance of

Dr. N.K. Verma

Professor of Physics

School of Physics and Materials Science

Thapar University

Patiala (Punjab) – 147004

July 2010

Dedicated

To All

My well Wishers

Certificate

This is to certify that report entitled "**Investigations on Diffuse Reflectance of Aluminium Doped Titania**" submitted by **Meenu,** Roll No. **300804015**, student of M.Sc. (Physics), Thapar University, Patiala, was carried out by her under my supervision. She has not submitted this material for the credit towards any other degree at Thapar University, Patiala or at any other university.

(N. K. Verma)

Supervisor
Professor
School of Physics & Materials Science
Thapar University
Patiala

(O. P. Pandey)

Professor and Head
School of Physics & Materials Science
Thapar University
Patiala

(R. K. Sharma) 23/7/10

Dean of Academic Affairs
Thapar University
Patiala

iii

Acknowledgement

Words often fail to express one's inner feeling of indebtedness and in fact words are not the proper media for this purpose. It is difficult to enunciate in words the deep sense of gratitude which I have for my esteemed supervisor **Professor N. K. Verma**, Thapar University, Patiala, for his support and precious guidance.

I take this opportunity to thank **Mr. Sanjeev Kumar**, research scholar for his critical and timely suggestions and immense encouragement. I also have deep gratitude towards him, for never turning down any query.

I also thank Mr. Gurmeet Singh and Ms. Manveen Kaur, research scholars for their timely cooperation throughout the duration of the project.

Special thanks to my lab mate Simanpreet Kaur for helping me out whenever I needed. I can never forget her support and encouragement.

For technical help, I want to thank Mr. Purushottam Singh and and Mr. Dinesh Thapar University, Patiala.

Last but not the least I would like to thank faculty of the Department, specially Dr. O. P. Pandey, Head, School of Physics and Material Science, Thapar University, Patiala, my family and friends for having supported me and encouraged me to work hard, without which this could not be possible.

(Meenu) 15/7/10

Abstract

Uniform nanosized anatase and rutile phase titania nanoparticles doped with aluminium were synthesized by sol-gel technique using titania isopropoxide as a starting precursor. The influence of various sol-gel conditions and dopant concentrations on the formation, phase, morphology and diffuse reflectance of NPs have been investigated and tentatively discussed. XRD studies clearly showed the formation of anatase and rutile phase of titania and also confirms that Al is not incorporated into the lattice of titania as no impurity peak of Al was found. EDX results confirm the presence of Al on the surface of titania. TEM and SEM micrograph show the uniformity in shape and size of synthesized nanoparticles. From the absorption spectra the band gap of the NPs was calculated and found to be higher than that of the bulk counterpart. The luminescence property of the NPs was studied by the emission spectrum, which confirms the presence of defect levels caused by the oxygen vacancies. The reflectance spectra of doped NPs calcined at 500^0C shows 97-99% reflectance as compared to uncalcined undoped NPs having 91-99% reflectance for the visible region.

CONTENTS

Chapter 1

Introduction

1.1 Introduction to Nanotechnology

1.1.1 History

The first observation and size measurement of nanoparticles was made in 1914 by Richard Adolf Zsigmondy who made a detailed study of gold sols and other nanomaterials with sizes down to 10 nm and less. He used ultra microscope that employs the dark field method for seeing particles with sizes much less than light wavelength. In the 1920s, Irving Langmuir and Katharine B. Blodgett introduced the concept of a monolayer. The topic of nanotechnology was again touched upon by "There's Plenty of Room at the Bottom," a talk given by physicist Richard Feynman on December 29, 1959. Feynman described a process by which the ability to manipulate individual atoms and molecules might be developed, using one set of precise tools to build and operate another proportionally smaller set, so on down to the needed scale. In the course of this, he noted, scaling issues would arise from the changing magnitude of various physical phenomena where gravity would become less important, surface tension and Van-der Waals attraction would become more important. In 1965 Gordon Moore observed that silicon transistors were undergoing a continual process of scaling downward, an observation which was later codified as Moore's law. Since his observation transistor minimum feature sizes have decreased from 10 micrometers to the 45-65 nm range in 2007. The term "nanotechnology" was first defined by Norio Taniguchi in 1974 as nano-technology mainly consists of the processing of separation, consolidation, and deformation of materials by one atom or molecule. In the 1980s the idea of nanotechnology as deterministic, rather than stochastic, handling of individual atoms and molecules was conceptually explored in depth by Dr. K. Eric Drexler, who promoted the technological significance of nano-scale phenomena and devices through speeches [1].

1.1.2 Nanotechnology

Nanotechnology is regarded as the key technology which will not only influence the development in near future but also have economic, social and ecological implications [2]. Nanotechnology is the world of miniature where everything is consider on the nanoscale terms. The most marvelous aspect is the boundless possibility for innovation,

nanotechnology can bring. It is still early stage but is rapidly building to be one of corner stone of modern technology whether it is electronics to medicine [3]. Nanotechnology should be separated from the term nanoscience. Nanotechnology is a blanket term which includes any number of methods which scientists have developed toward the goal of manipulating matter at an atomic and sub-atomic level, whereas nanoscience is what the study of this manipulation [4].

1.1.3 Nanoscale

The nanoscale derives from the word "nano" or billionth of a meter, but means something broader. Nanoscale refers to anything which has the characteristic size of its defining property as nanometer or from 0.1 nm to 100 nm (fig.1.1). This range refers to the atomic and molecular domain, which is where the nanoscale action is [5].

- A human hair is about 50,000 -100,000 nanometers across.
- Nanometer is about 10 - 15 hydrogen atoms next to each other
- Viruses are typically 75 times bigger than a nanometer.
- A molecule of DNA is ~ 2.5 nanometers wide.
- A nanometer is to a foot what one foot is to 4,800 miles.

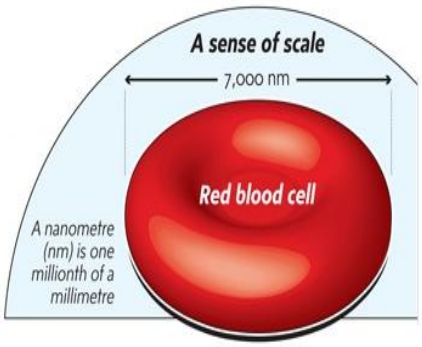

Fig. 1.1 Red Blood Cell (~7 microns)

1.1.4 Change in Properties at Nanoscale

Laws relating to physical, chemical, biological, electrical, magnetic and other properties at the nano-scale are different from those that apply to macro matter; as it is laws of quantum mechanics that apply at that scale. Attempts to achieve control over

conductivity, opacity, strength, ductility, reactivity, etc. in different combinations of matter, are among the earliest of research forays in this field. A whole new world is opening up, in which things that are made are not only just smaller, but stronger, or faster or cheaper or better in terms of so many features that were unthinkable, leading to the creation of whole new capabilities, new products and new markets [6].

At nanoscale the properties that changes are:-

a. Electrical:-

- Optimized electron conductivity through carbon nanotubes and nano structured superconductors
- Electric insulators through nano structured fillers in components of high voltage power lines

b. Optical:-

- Optimized light absorption properties of solar cells through quantum dots and nanolayers in stack cells
- Anti reflection properties for solar cells to increase energy yield of solar cells
- Luminescent polymers for production of energy efficient organic light diodes

c. Chemical:-

- More efficient catalysis in fuel cells or for the chemical conversion of fuels through extended surfaces and specific catalyst design
- More powerful batteries, accumulators and supercapacitors through higher specific electrode surfaces

d. Mechanical:-

- Improved strength of construction materials for rotor blades of wind power plants
- Wear resistant nanolayers for drill probes, gear boxes and engine components

e. Thermal:-

- Nano structured heat protection layers for turbine blades in gas and aircraft turbines
- Improved heat conductivity of carbon nanotubes for optimized heat exchangers **[7]**

1.1.5 Why Do Properties Change At Nanoscale?

The transition from microparticles to nanoparticles can lead to a number of changes in physical properties. The major factors in this are the increase in the ratio of the surface area to volume, and the size of the particle moving into the realm where quantum effects predominate.

Important ways in which nanoscale materials may differ from macro scale materials

a) Quantum confinement
b) Greater surface area to volume ratio

a) Quantum Confinement

Quantum confinement effect can be observed once the diameter of the particle is of the magnitude as the wavelength of electron wave function [8]. When the materials are so small, their electronic and optical properties deviate substantially from those of bulk materials. A particle behaves as if it were free when the confining dimension is large compared to the wavelength of the particle. During this state, band gap remains at its original energy due to continuous energy state (fig.1.2). However, as the confining dimension decreases and reaches a certain limit typically in nanoscale the energy spectrum turns to discrete. As a result bandgap becomes size dependent. This ultimately results a blue shift in optical illumination as the size of the particles decreases. This effect describes the phenomenon results from electrons and electron holes being squeezed into a dimension that approaches a critical quantum measurement, called the exciton Bohr radius. In current application, a quantum dot confines in all three dimensions such as a small sphere.

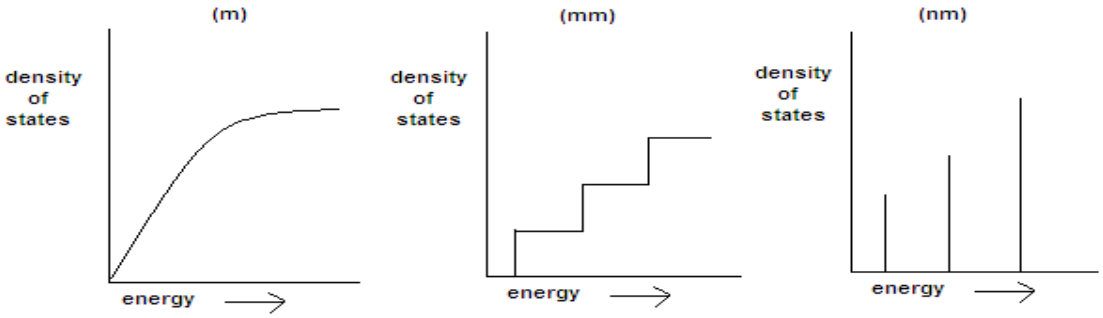

Fig. 1.2 The energy levels become discrete at nanoscale

b) Surface to Volume Ratio

The increase in surface to volume ratio, which is gradual progression as the particle gets smaller (fig. 1.3), leads to an increasing dominance of the behavior of atoms on the surface of the particle over that those in the interior of the particle [9]. This affects both the properties of the particle in isolation and its interaction with other materials. High surface area is a critical factor in performance of catalysis.

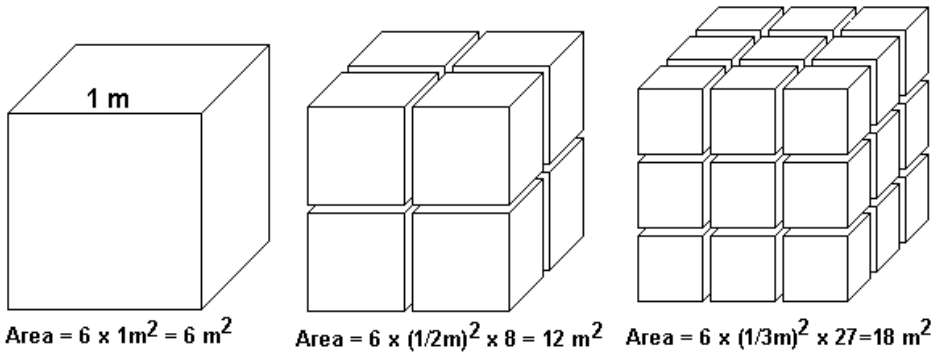

Fig. 1.3 Surface to volume ratio increases at nanoscale

1.1.6 Applications

The various applications which nanotechnology has been impacting are indicated in Figure 1.4

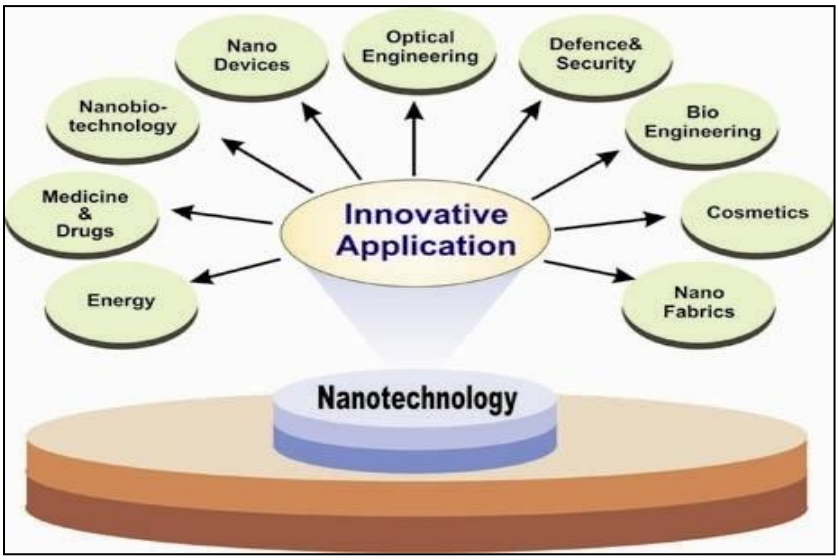

Fig 1.4 Applications of nanotechnology [10]

1.2 Synthesis Methods

There are two distinct approaches for making nanostructures, which can be characterized as top-down and bottom-up.

Top-down approach

A top-down approach (is also known as step-wise design) is essentially the breaking down of a system to gain insight into its compositional sub-systems. Production processes by using Top-down approaches are:

- High energy milling
- Chemical mechanical milling
- Vapour phase condensation
- Electro-explosion

  Sputtering

Bottom-Up Approach

"Bottom-up" approach refers to the build-up of a material from the bottom: atom-by-atom, molecule-by-molecule or cluster-by-cluster. The colloidal dispersion is a good example of bottom-up approach in the synthesis of nano-particles. Nanolithography or nanomanipulation is commonly a bottom-up approach.

- Sol-gel
- Solvothermal/Hydrothermal
- CVD/MOCVD
- MBE
- Seed Growth method

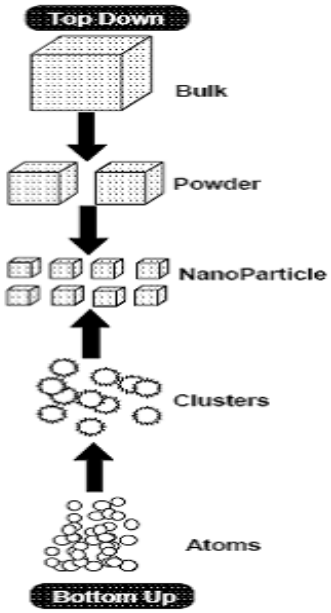

Fig. 1.5 Two approaches for synthesis

1.3 Reflectance

1.3.1 Introduction to Reflectance

The phenomenon of bending of light when it strikes the boundary of the material is called reflection. The reflectance spectrum or spectral reflectance curve is the plot of the reflectivity as a function of wavelength. Reflectivity is distinguished from reflectance by the fact that reflectivity is a value that applies to thick reflecting objects. When reflection occurs from thin layers of material, internal reflection effects can cause the reflectance to vary with surface thickness. Reflectivity is the limit value of reflectance as the surface becomes thick [11].

For most materials, the majority of the light that is not absorbed is reflected from the surface, and thus a material's surface reflectance properties are surely some of its most important optical attributes [12]. When light is reflected from a surface, it is generally scattered in many directions, producing a pattern that is characteristic of the material. Variation in the distribution of scatter gives rise to such varied visual appearances as gloss paint, and gold [13].

1.3.2 Types of reflectance

The amount of light reflected by an object, and how it is reflected, is highly dependent upon the smoothness or texture of the surface [14]. Depending upon surface type there are two types of reflections.

a. Specular reflection

Specular reflection is defined as light reflected from a smooth surface at a definite angle (fig.1.6) [15]. For the specular reflection to occur following conditions are required:-

- The angle of the reflected ray is the same as that of the incident ray.
- The reflected ray lies in the plane containing the incident ray and the normal line. This plane is known as the plane of incidence.

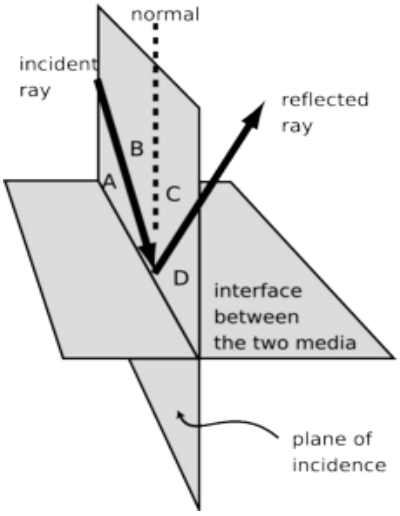

Fig 1.6 Specular reflection **[16]**

b. <u>Diffuse reflectance</u>

Diffuse reflection is uniform reflection of light with no directional dependence for the viewer. Diffuse reflection originates from a combination of internal scattering of light, i.e. the light is absorbed and then re-emitted, and external scattering from the rough surface of the object [17]. .

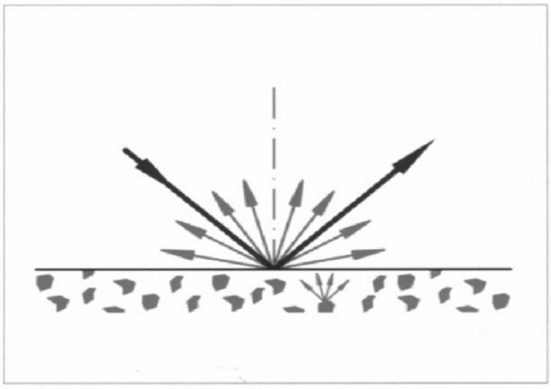

Fig 1.7 Diffuse reflection **[18]**

For each type of reflection, each individual ray follows the law of reflection. However, the roughness of the material means that each individual ray meets a surface which has a different orientation [19]. The normal line at the point of incidence is different for different rays. Subsequently, when the individual rays reflect off the rough surface according to the law of reflection, they scatter in different directions.

1.3.3 Reflective coating:-

These are the chemicals that selectively absorb and reflect different spectra of light. When a surface is coated with a pigment, light hitting the surface is reflected, minus some wavelengths [20]. This subtraction of wavelengths produces the appearance of different colors. Most reflective coatings are a blend of several chemical pigments, intended to produce a reflection of a given color. Rayleigh scattering is re-radiation that does not obey law of reflection in which the angle of incidence equals the angle of reflection [21]. When the size of the object is very small in relation to the wavelength of the incident wave, the scattered wave front exhibits several relevant properties. These are: (1) the scattered wave front propagates equally in all directions. This propagation is said to be isotropic. (2) The amplitude of the scattered wave front varies inversely with the fourth power of the wave length of the incident wave.

1.3.3.1 Components of reflective coating: -

a. Pigment:-

Pigments are granular solids incorporated into the coating to contribute color, toughness, texture or simply to reduce the cost of the coating. Hiding pigments in making coating opaque protect the substrate from the harmful effects of ultraviolet light. Hiding pigments include titanium dioxide, phthalo blue, red iron oxide etc.

b. Binder: -

The binder is the actual film forming component of coating. It is the only component that must be present; other components are included optionally, depending on the desired properties of the cured film. The binder imparts adhesion, binds the pigments together, and strongly influences properties such as gloss potential, exterior durability, flexibility, and toughness.

c. Solvent: -

The main purposes of the solvent are to adjust the curing properties and viscosity of the coating. It is volatile and does not become part of the coating film. It also controls flow and application properties, and affects the stability of the coating while in liquid state. Its main function is as the carrier for the non volatile components

d. Additives:-

Besides the three main categories of ingredients, coating can have a wide variety of miscellaneous additives, which are usually added in very small amounts and yet give a very significant effect on the product [22].

1.3.5 Reflective materials: -

Different nanoparticles that are used in reflective coatings are TiO_2, ZnO, Al_2O_3, fumed silica and ZrO_2. These materials have high refractive index that's why these are used in coatings. Titania has highest refractive index of any material known to man even greater than diamond. It gives to coating high hiding power, meaning the ability to mask or hide a substrate. It does this more effectively than any other white pigment. Today, titanium dioxide pigment is by far the most important material used in the coatings and plastics industry for whiteness and opacity [23].

Chapter 2

Material And Characterization

2.1 Material

2.1.1 Titania

Titanium dioxide is a wide band gap (Eg=3.2 eV) semiconductor material. It is extensively used as photocatalyst as well as in solar cells. Numerous research papers on TiO_2 indicate that there are many reasons to investigate TiO_2. It can be used in oil and air purification. It is useful in nitrogen fixation as well as dissociation of water molecules to produce hydrogen gas. Titanium minerals are used in the production of titanium dioxide pigment. Pure white, highly refractive, ultra violet absorbing, non toxic and inert, titanium pigments are used in protective coatings, such as house and car paints, sunscreens, plastics, paper and textiles, as well as a growing number of foodstuffs and cosmetics. It is therefore not surprising that investigation of TiO_2 nanoparticles also has been focus of intense research activity [24].

2.1.1.1 Background

Pure titanium dioxide does not occur in nature but is derived from ilmenite or leuxocene ores. It is also readily mined in one of the purest forms, rutile beach sand. These ores are the principal raw materials used in the manufacture of titanium dioxide pigment.

2.1.1.2 Key Properties

Atomic Structure of Titanium

- Atomic number: 22
- Atomic Radius: 2Å
- Atomic Volume: 10.64cm^3/mol
- Covalent Radius: 1.32Å
- Crystal Structure: Hexagonal
- Electron Configuration:$1s^2\ 2s^2 2p^6\ 3s^2 3p^6 4s^2 3d^2$
- Electrons per Energy Level: 2,8,10,2
- Ionic Radius: 0.605Å
- Filling Orbital: $3d^2$
- Number of Electrons (with no charge): 22

- Number of Neutrons (most common/stable nuclide): 26
- Number of Protons: 22
- Oxidation States: 4
- Valence Electrons: $4s^2$ $3d^2$

Chemical Properties of Titanium

- Electrochemical Equivalent: 0.4468g/amp-hr
- Electron Work Function: 4.33eV
- Electronegativity: 1.54 (Pauling scale); 1.32 (Allrod Rochow scale)
- Heat of Fusion: 15.45kJ/mol
- Incompatibilities:
- Ionization Potential
    - First: 6.82
    - Second: 13.58
    - Third: 27.491
- Valence Electron Potential (-eV): 95.2

Physical Properties of Titanium

- Atomic Mass Average: 47.88
- Boiling Point: 3560K
- Density: 4.54g/cc
- Elastic Modulus:
    - Bulk: 108.4/GPa
    - Rigidity: 45.6/GPa
    - Youngs: 120.2/GPa
- Enthalpy of Atomization: 468.6 kJ/mole
- Enthalpy of Fusion: 15.48 kJ/mole
- Enthalpy of Vaporization: 429 kJ/mole
- Heat of Vaporization: 421kJ/mol
- Melting Point: 1933K
- Molar Volume: 10.64 cm^3/mole
- Physical State (at 20°C & 1atm): Solid

- Specific Heat: 0.52J/gK
- Vapor Pressure = 0.49Pa [25]

2.1.1.3 Phases of titania

Titanium dioxide occurs as well-known minerals rutile, anatase and brookite. The most common form is rutile, which is also the most stable form. Anatase and brookite both convert to rutile upon heating. Rutile, anatase and brookite all contain six coordinated titanium.

Rutile has among the highest refractive indices of any known mineral and also exhibits high dispersion. Rutile derives its name from the Latin rutilus, red, in reference to the deep red color observed in some specimens when viewed by transmitted light [26].

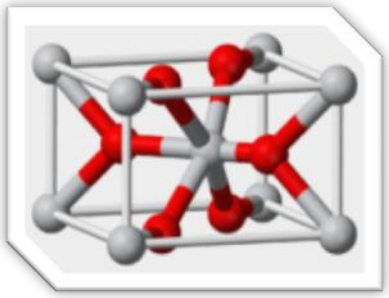

Rutile

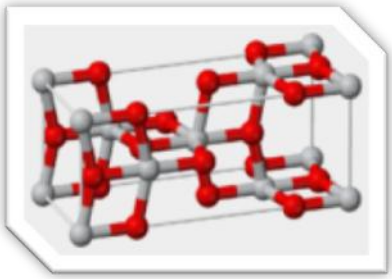

Anatase

Anatase is always found as small, isolated and sharply developed crystals, and like rutile, a more commonly occurring modification of titanium dioxide, it crystallizes in the tetragonal system but although the degree of symmetry is the same for both, there is no relation between the interfacial angles of the two minerals [27].

Applications:-Widely used in plastics, superb industrial paints, gloss emulsion paints, high quality paper coatings, waxing stocks and rubber flooring.

2.1.2 Effect of doping

TiO_2 based materials have been widely used as pigment, hydrogen production, self-cleaning surfaces, antibacterial materials, degradation of organic compounds in polluted air and wastewater, solar cells and fuel cells. However, because of the high bandgap

energy of TiO_2, it is limited to the response of ultraviolet (UV) light and a large fraction of solar energy cannot be utilized. Thus, great attempts have been made to improve the efficiency of TiO_2 by enhancing the absorption of visible light. With doping its properties get enhanced and doped-titania is useful in many industrial applications [28].

2.1.3 Applications

A.) Pigments

The most important function of titanium dioxide is in powder form as a pigment for providing whiteness and opacity to such products such as paints and coatings, plastics, paper, inks, fibers and food and cosmetics. The high refractive index and bright white color of titanium dioxide make it an effective opacifier for pigments. The material is used as an opacifier in glass and porcelain enamels, cosmetics, sunscreens, paper, and paints.

B.) Photo catalysis

Titania acts as a photosensitize for photovoltaic cells, and when used as an electrode coating in photo electrolysis cells can enhance the efficiency of electrolytic splitting of water into hydrogen and oxygen.

C.) Oxygen Sensors

Even in mildly reducing atmospheres titania tends to lose oxygen and become sub stochiometric. In this form the material becomes a semiconductor and the electrical resistivity of the material can be correlated to the oxygen content of the atmosphere to which it is exposed. Hence Titania can be used to sense the amount of oxygen present in an atmosphere.

D.) Antimicrobial Coatings

The photo catalytic activity of titania results in thin coatings of the material exhibiting self cleaning and disinfecting properties under exposure to UV radiation. These properties make the material a candidate for applications such as medical devices, food preparation surfaces, air conditioning filters, and sanitary ware surfaces [29].

2.1.4 Properties of aluminum

Aluminium is a very light metal with a specific weight of 2.7 g/cm^3, about a third that of steel. Aluminium is a good reflector of visible light as well as heat, and that together with its low weight, makes it an ideal material for reflectors in, for example, light fittings or rescue blanket. Aluminium naturally generates a protective oxide coating and is highly corrosion resistant. It is particularly useful for applications where protection and conservation are required [30].

2.2 Characterization techniques

2.2.1 X-Ray Diffraction

About 95% of all solid materials can be described as crystalline. When X-rays interact with a crystalline substance one gets a diffraction pattern. In 1919 A.W. Hull gave a paper titled, "A New Method of Chemical Analysis". He pointed out that "every crystalline substance gives a pattern; the same substance always gives the same pattern; and in a mixture of substances each produces its pattern independently of the others". The X-ray diffraction pattern of a pure substance is like a fingerprint of the substance. The powder diffraction method is thus ideally suited for characterization and identification of polycrystalline phases [31].

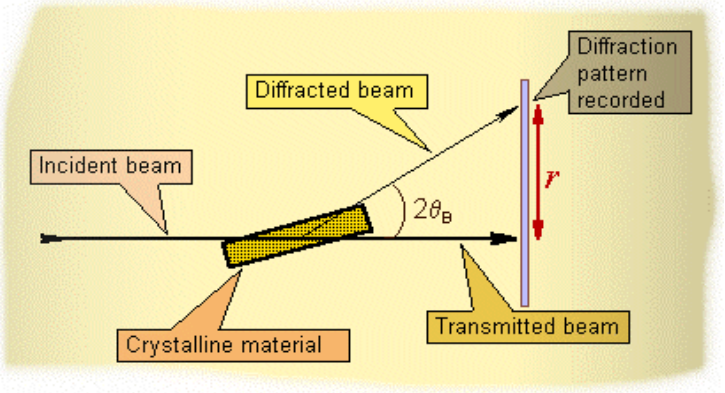

Fig 2.1 Basic principle of XRD

Basic principle

X-ray diffraction is based on constructive interference of monochromatic X-rays and a crystalline sample.

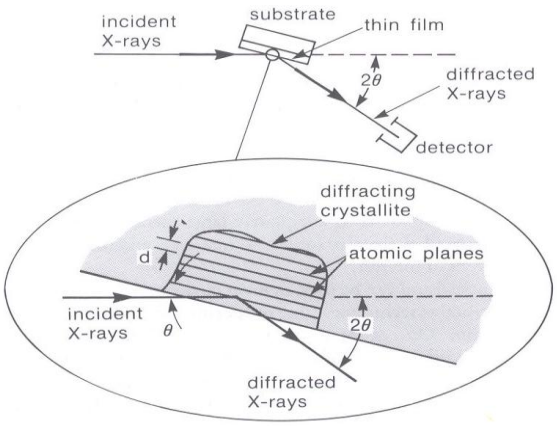

Fig 2.2 Diffraction at Bragg's angle

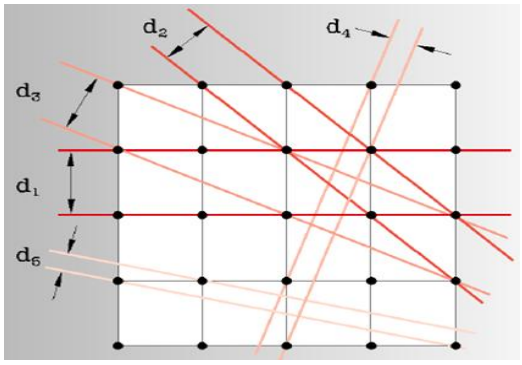

Fig 2.3 Reflecting planes in cubic crystal

The X-rays are directed toward the sample. The interaction of the incident rays with the sample produces constructive interference when conditions satisfy Bragg's Law ($n\lambda=2d$ sin θ). This law relates the wavelength of electromagnetic radiation to the diffraction angle and the lattice spacing in a crystalline sample [32].

Data analysis

Example of an X-ray powder diffractogram produced during an X-ray scan. The peaks represent positions where the X-ray beam has been diffracted by the crystal lattice. The set of *d*-spacing's which represent the unique "fingerprint" of the mineral can easily be calculated from the 2-theta values by Scherer equation [33]. Full width at half maximum of XRD pattern was used along with Scherer's equation to estimate mean particle (grain) size. The equation is given by:-

$$d = 0.9\,\lambda / \beta\cos\theta$$

Where d is mean diameter of nanoparticles; λ is the wavelength of X-ray radiation source; β is the angular full width at half maximum of X-ray diffraction peak at diffraction angle θ. The use of degrees 2-theta in depicting X-ray powder diffraction scans is a matter of convention and can easily be related back to the geometry of the instrument.

XRD has a wide range of applications in geology, material science, environmental science, chemistry, Forensic science and the pharmaceutical industry.

- Measure the average spacing between layers or rows of atoms

- Determine the orientation of a single crystal or grain
- Find the crystal structure of an unknown material
- Measure the size, shape and internal stress of small crystalline regions [34].

2.2.2 Transmission electron microscopy

The use of electron diffraction to solve crystallographic problems was pioneered in the Soviet Union by B.K.Vainshtein and his colleagues as early as the 1940s.

Basic principle

A Transmission Electron Microscope is similar in design to an ordinary light microscope with one key difference: instead of using light, it uses electrons [35].

Diffracted waves scattered by the atomic potential form diffraction spots on the back focal plane after being focused with the objective lens [36]. The diffracted waves are recombined to form an image on the image plane. The use of electromagnetic lenses allows diffracted electrons to be focused into a regular arrangement of diffraction spots that are projected and recorded as the electron diffraction pattern. If the transmitted and the diffracted beams interfere on the image plane, a magnified image of the sample can be observed. The space where the diffraction pattern forms is called reciprocal space, while the space at the image plane or at a specimen is called real space. The transformation from the real space to the reciprocal space is mathematically given by the Fourier transform.

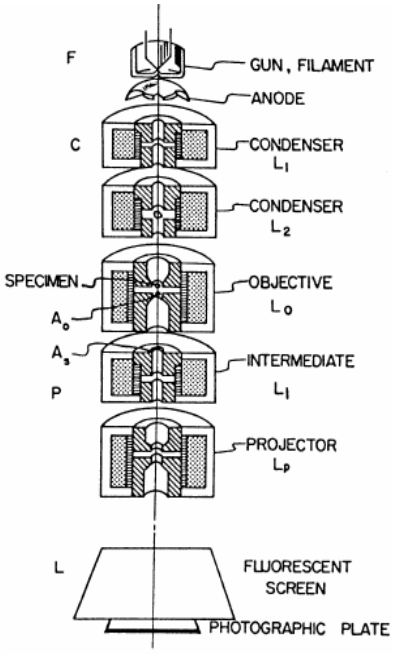

Fig 2.4 Schematic Diagram

A great advantage of the TEM is in the capability to observe, by adjusting the electron lenses, both electron microscope images (information in real space) and diffraction patterns (information in reciprocal space) for the same region.

Mechanisms of image formation:-

In TEM the specimen is transparent for electrons; absorption of electrons plays a minor role in image formation [37]. Deflection mechanism (scattering and diffraction of electrons) is mainly responsible for image formation.

- Mass-thickness contrast (biology and polymer specimen)
- Diffraction contrast (major image formation mechanism)
- Phase contrast (high resolution image of crystal lattice)

2.2.3 Energy Dispersive X-ray Spectroscopy

Energy dispersive X-ray spectroscopy (EDS) is an analytical technique used for the elemental analysis or chemical characterization of a sample. As a type of spectroscopy, it relies on the investigation of a sample through interactions between electromagnetic radiation and matter, analyzing x-rays emitted by the matter in response to being hit with charged particles. Its characterization capabilities are due in large part to the fundamental principle that each element has a unique atomic structure allowing x-rays that are characteristic of an element's atomic structure to be identified uniquely from each other [38].

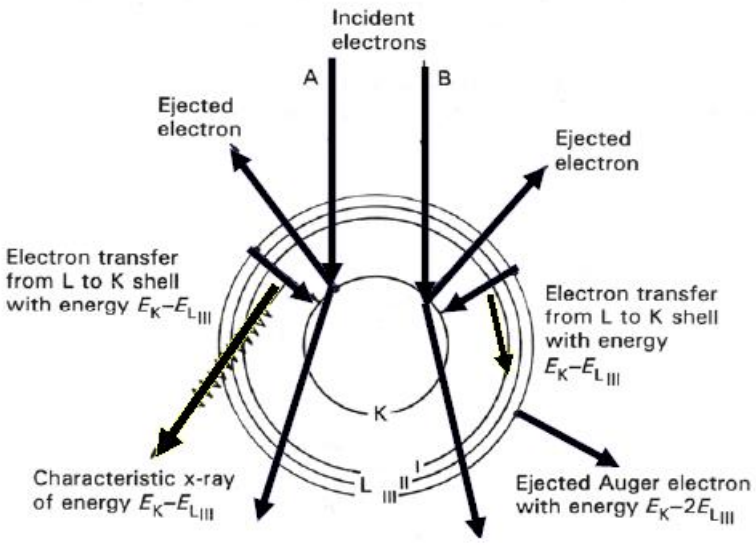

Fig 2.5 The emission of characterstic X-ray by e^- A and emission of augar electron by e^- B

To stimulate the emission of characteristic X-rays from a specimen, a high energy beam of charged particles such as electrons or protons or a beam of X-rays, is focused into the sample being studied. At rest, an atom within the sample contains ground state electrons in discrete energy levels or electron shells bound to the nucleus [39]. The incident beam may excite an electron in an inner shell, ejecting it from the shell while creating an electron hole where the electron was. An electron from an outer, higher-energy shell then fills the hole, and the difference in energy between the higher-energy shell and the lower energy shell may be released in the form of an X-ray. The number and energy of the X-rays emitted from a specimen can be measured by an energy dispersive spectrometer. As the energy of the X-rays is characteristic of the difference in energy between the two shells, and of the atomic structure of the element from which they were emitted, this allows the elemental composition of the specimen to be measured.

Uses

The positions of lines (peaks with appropriate energies) give information about the qualitative composition of the sample. The number of the X-ray quanta is the measure for the concentration of the elements (peak-height). There is not linear connection between quantum numbers and concentration portions of the elements. The concentration calculation needs the net count rates or from it derived measured variables.

2.2.4 UV-Visible Spectroscopy

UV-Visible spectroscopy is the measurement of the attenuation of the beam of light after passes through a sample or after reflection from a sample surface [40]. UV-Visible spectroscopy includes a variety of absorption, transmittance and reflectance measurements in UV, visible and near-IR. These measurements can be at a single wavelength or over an extended spectral range.

Principle

Ultraviolet-visible spectroscopy measures the attenuation of light passes through a sample or is reflected from a sample surface. The attenuation can result from absorption, scattering and reflection. The cause of the attenuation is often not important for many

optical materials and the total resulting transmittance or reflectance is sufficient to determine the suitability of a material for certain application.

Experimental measurements are made in terms of transmittance T:

$$T = P/P_0$$

Where P is the radiant power after it passes through the sample and P_0 is the initial radiant power. This relationship will also be found in terms of light intensities:-

$$T = I/I_0$$

Beer-Lambert law: - The absorbance of light is directly proportional to the distance light travels through the sample and to the concentration of the absorbing species.

Measured Absorbance $A= a.b.c$

a: wavelength dependent absorptive coefficient

b: path length

c: analyte concentration

Also $A= -\log T = -\log (P/P_0)$

Uses

In organic molecules and polymers, the UV-Vis spectrum can help to identify chromophores and the extent of electronic delocalization. For inorganic complexes the UV-Vis spectrum can provide information about oxidation states, electronic structures and metal-ligand interactions.

For solid materials, the UV-Vis spectrum can measure the band-gap and identify any localized excitations or impurities.

2.2.5 Photoluminescence

All solids, including semiconductors have so-called “energy gaps” for the conducting electrons. If a light particle (photon) has energy greater than the band gap energy, then it can be absorbed and thereby raise an electron from the valence band up to the conduction band across the forbidden energy gap. In this process of photoexcitation, the electron generally has excess energy which it loses before coming to rest at the lowest energy in the conduction band. At this point the electron eventually falls back down to the valence band. As it falls down, the energy it loses is converted back into a luminescent photon which is emitted from the material. Thus the energy of the emitted photon is a direct

measure of the band gap energy, Eg. The process of photon excitation followed by photon emission is called photoluminescence [41].

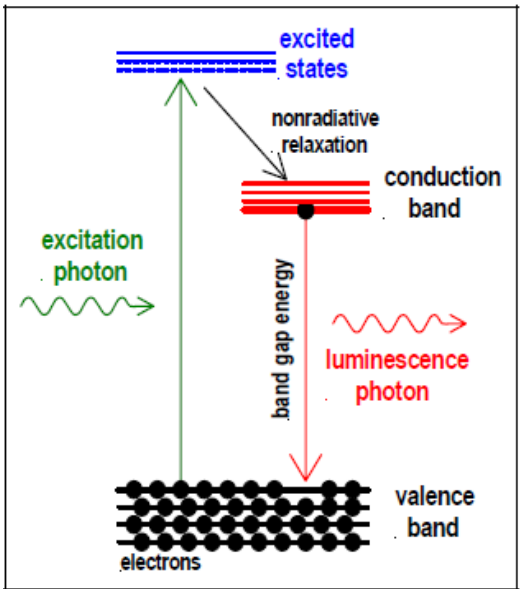

Fig 2.6 Basic principle of PL

The PL spectrum provides the transition energies, which can be used to determine electronic energy levels. The PL intensity gives a measure of the relative rates of radiative and non-radiative recombination. Variation of the PL intensity with external parameters like temperature and applied voltage can be used to characterize further the underlying electronic states and bands.

Types of photoluminescence

The simplest photoluminescent processes are resonant radiations, in which a photon of a particular wavelength is absorbed and an equivalent photon is immediately emitted.
This is of two types:-

a. **Fluorescence**:-The chemical substrate undergoes internal energy transitions before reemitting the energy from the absorption event. This is also typically a fast process, but in this some of the original energy is dissipated so that the emitted light photons are of lower energy than those absorbed

b. **Phosphorescence**:-The energy from absorbed photons undergoes intersystem crossing into a state of higher spin multiplicity, usually a triplet state. Once the energy is trapped in the triplet state, transition back to the lower singlet energy states is quantum mechanically forbidden. This results in a slow process of radiative transition back to the singlet state.

Uses of Photoluminescence

The most common radiative transition in semiconductors is between states in the conduction and valence bands, with the energy difference being known as the band gap. Band gap determination is particularly useful when working with new compound semiconductors. Radiative transitions in semiconductors also involve localized defect levels. The photoluminescence energy associated with these levels can be used to identify specific defects, and the amount of photoluminescence can be used to determine their concentration [42].

2.4 Literature Review

Titanium dioxide (TiO_2) is one of the most extensively studied transition metal oxides and has gained wide use in a variety of technological applications. A. Borkowska *et al*.has studied that Lanthanide-doped luminescent materials have been intensively studied because of their possible applications in photoelectric devices and optical communication fields. TiO_2 has been used as the favorable host material for rare earth elements, due to its outstanding optical and thermal properties and high stability [43]. Synthesis and characterization of titania nanoparticles has been carried out by many researchers in general. Y. Zhu *et al.* prepared nanosized TiO_2 powder with anatase structure by a sol-gel method using $TiCl_4$ ethanol solution as a precursor [44]. They promoted the formation of anatase TiO_2 by increasing gelatinizing time. They studied the influence of alcohol on the reacting progress and dispersivity. The size and activity of alcohol molecule were found to have influence on the polymerization and mineralization degree of the precursor and the dispersivity of TiO_2 powders. G. Facchin *et al.* prepared a set of TiO_2 and Pt-TiO_2 polycrystalline samples by sol-gel method and hydrolyzing a modified alkoxide titanium precursors under acidic conditions [45]. They characterized the sample using several

techniques, namely thermogravimetric analysis, X-ray diffraction coupled with a Rietveld refinement procedure, X-ray photoelectron spectroscopy and determination of specific surface area. Characterization results indicated that the thermal and chemical treatments of the catalysts influenced the photocatalytic activity. P. H. Borse *et al.*TiO_2 nanoparticles synthesized at room temperature using a simple chemical precipitation route [46]. Wide-angle X-ray scattering and transmission electron microscopy confirmed that "as-synthesized" particles as well as annealed particles are nanoparticles having pure rutile phase. They determined the purity and composition of the particles using energy dispersive analysis of X-rays and X-ray photoelectron spectroscopy, respectively. S. Mayadevi *et al.* synthesized titania powder using chemical precipitation [47]. They employed XRD, DTA/TGA/DTG techniques for phase analysis and to know the thermal changes taking place in precipitated precursor during heating. A. V. Muruganc *et al*. obtained nanocrystalline titanium dioxide in the anatase phase using urea and $TiOCl_2$ by microwave hydrothermal method [48]. X-ray diffraction studies on these oven-dried powders indicated the formation of single phase anatase. Transmission electron microscopy investigations revealed the average particle size of these powders to be 10 nm. X. Ding *et al.* prepared titania nanoparticles with and without alumina dopant by a sol-gel method [49]. They investigated influence of a small amount of alumina dopant on the structural changes. XRD analysis showed that phase transformation from anatase to rutile occurred for annealing temperatures above 823 K and was completed at 1073 K. On the other hand, the alumina-doped TiO_2 gel remained amorphous after annealing at 623 K for 2 h. When the annealing temperature was 723 K, crystallization began, and the phase transformation from anatase to rutile did not occur until the annealing temperature was elevated to 1073 K. S. Liu *et al*. fabricated aluminium doped TiO_2 mesoporous material by solid-state reaction [50]. X-ray diffraction, high resolution transmission electron microscopy and energy dispersive spectroscopy ultraviolet visible light spectroscopy and X-ray photoelectron spectroscopy showed that the mesoporous architecture of aluminium-doped TiO_2 was composed of crystal wall and micro-/mesopore formed gradually by the mesopore degradation of anatase TiO_2. The results showed that a small quantity of aluminium doped into anatase TiO_2 could improve photodegradation activity, and the photodegradation activity of aluminium doped TiO_2

was higher than that of pure TiO_2. S. Perera *et al.* have done the solid-state hydrolysis and air calcination of aluminum-doped $TiCl_3$ which leads to crystalline anatase TiO_2 that is stable on heating to 1000 °C [51]. Particle and crystallite sizes are at or above 100 nm, which is much larger than sizes observed for unstabilized anatase TiO_2 systems. M.A. Behnajady *et al*. prepared silver doped TiO_2 nanoparticles by liquid impregnation (LI) and photodeposition (PD) methods [52]. Scanning electron micrographs and XRD results showed that the silver doped TiO_2 is more efficient than undoped TiO_2 at photocatalytic degradation of AR88. The positive effect of silver on the photoactivity of TiO_2 at degradation of AR88 may be explained by its ability to trap electrons. Q.R. Deng *et al*. obtained V and Ga co-doped TiO_2 thin films by pulsed laser deposition (PLD) using sintered ceramic targets, followed by short term annealing at 1000 ^{0}C [53]. They characterized the structures of the thin films by X-ray diffraction (XRD) and investigated optical absorption properties of the films using UV–VIS spectrophotometer.

Chapter 3

Experimental Details

3.1 Sol-gel method

The sol-gel process, as the name implies, involves the evolution of inorganic networks through the formation of a colloidal suspension (sol) and gelation of the sol to form a network in a continuous liquid phase (gel). Sol-gel process paves the way to the versatility and ease of liquid film deposition on many types of substrates for a variety of inorganic and hybrid coatings materials [54]. The precursors for synthesizing these colloids consist usually of a metal or metalloid element surrounded by various reactive ligands. The starting material is processed to form a dispersible oxide and forms a sol in contact with water or dilute acid. Removal of the liquid from the sol yields the gel, and the sol/gel transition controls the particle size and shape. Calcination of the gel produces the oxide.

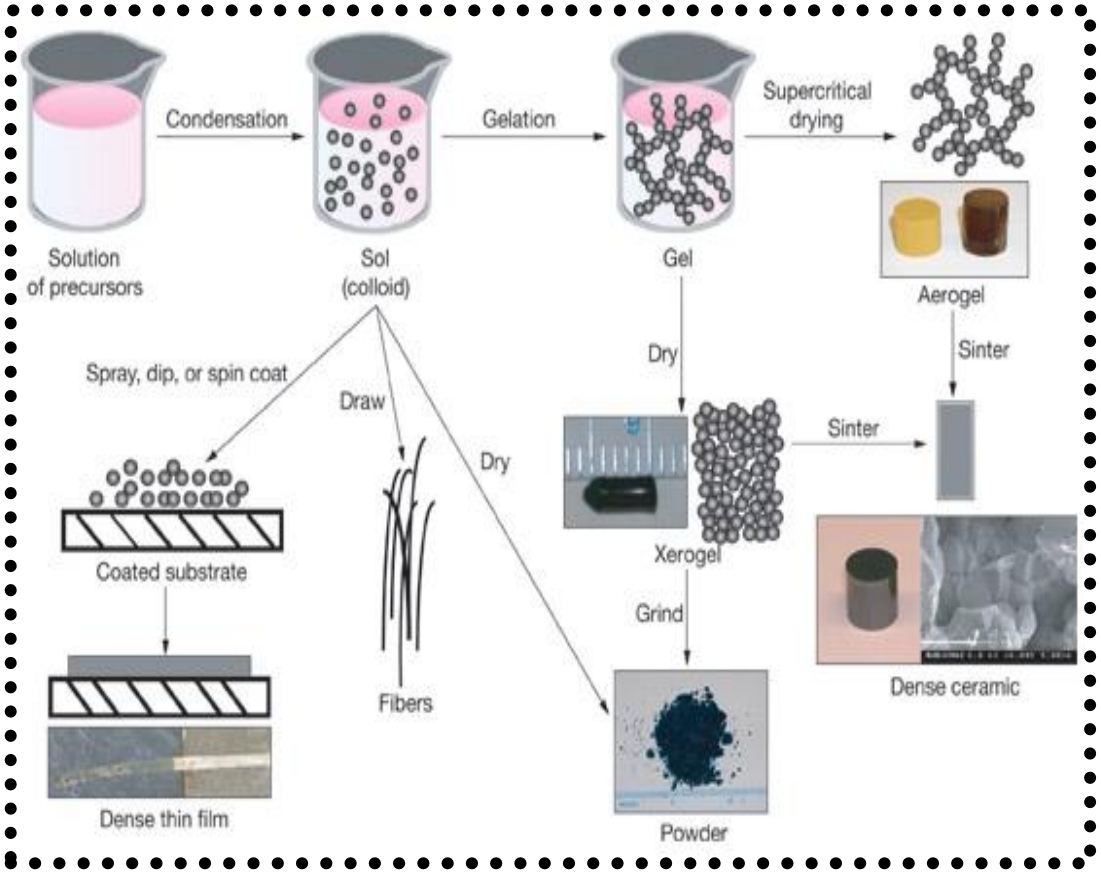

Fig 3.1 Schematic representation of sol-gel process

Sol-gel processing refers to the hydrolysis and condensation of alkoxide-based precursors such as tetraethyl orthosilicate [55]. The reactions involved in the sol-gel chemistry based on the hydrolysis and condensation of metal alkoxides M (OR)**z** can be described as follows:

$$MOR + H_2O \rightarrow MOH + ROH \text{ (hydrolysis)}$$

$$MOH + ROM \rightarrow M\text{-}O\text{-}M + ROH \text{ (condensation)}$$

There is densification and decomposition of the gels at high temperatures ($T>800^0C$). The pores of the gel network are collapsed, and remaining organic species are volatilized. Sol-gel method of synthesizing Nanomaterials is very popular amongst chemists and is widely employed to prepare oxide materials. The interest in this synthesis method arises due to the possibility of synthesizing nonmetallic inorganic materials like glasses, glass ceramics or ceramic materials at very low temperatures compared to the high temperature process required by melting glass or firing ceramics.

The major technical difficulties to overcome in developing a successful bottom-up approach is controlling the growth of the particles and then stopping the newly formed particles from agglomerating. The production rates of nano powders are very low by this process. The main advantage is one can get monosized nano particles by any bottom up approach [56].

3.2Synthesis

In present work, aluminum doped titania nanoparticles were prepared by sol gel process. The chemicals which have been used for the synthesis are titanium isopropoxide, 2-propanol and aluminium chloride as doping agent

The five samples were prepared with different molar concentration of dopant as given follow:-

1. Undoped titania
2. 0.01% Al_2Cl_3 of titania
3. 0.1% Al_2Cl_3 of titania

4. 1% Al_2Cl_3 of titania
5. 5% Al_2Cl_3 of titania

Procedure of synthesis

- Desired weight of Al_2Cl_3 was added to 50ml of 2-propanol
- 122.5ml of de-ionized water was added to 200ml of 2-propanol
- Both the samples were stirred for half an hour.
- After half an hour, the aluminum chloride solution was mixed in water solution and resulting solution was stirred for half an hour.
- Another sample of titanium isopropoxide in 200ml of 2-propanol was prepared and stirred for half an hour.
- After half an hour solution of aluminum + water was mixed dropwise in titanium solution.
- The resulting solution was stirred for 5hours.
- The white precipitates thus formed were filtered and washed several times with 2-propanol.
- The precipitates were then dried in an oven at 60^0C for 24hours. When the precipitates were completely dried, they were crushed to fine powder by grinding process.
- The powder thus formed was preserved in air tight container.

Chapter 4

Results And Discussion

4.1 X-ray diffraction study

Phase purity, crystal structure and crystallinity of titania powder can be estimated using x-ray diffraction diffractogram. Figure 4.1 shows the x-ray diffractogram of synthesized uncalcined titania powder. No peak was found which indicates the amorphous nature of titania powder [57]. A thermal treatment is necessary to improve the crystallinity of amorphous titania [58].

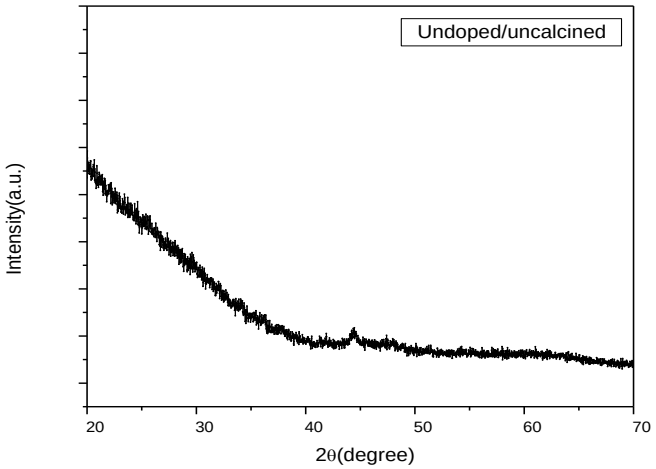

Figure 4.1 X-ray diffraction pattern of uncalcined titania

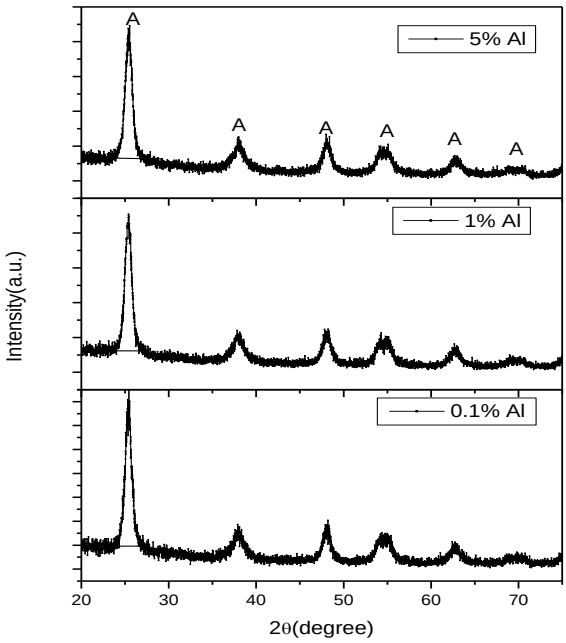

Figure 4.2:- X-ray diffraction spectra of Al-doped-TiO_2 at 500^0C temperature

Figure 4.2 shows the diffraction spectra of TiO_2 particles doped with 0.1, 1 and 5% aluminium. The crystalline phase of the doped titania particles was identified to be anatase form as compared with JCPDS card no. 21-1272. No peak corresponding to aluminium was found indicating that Al is not incorporated in TiO_2 lattice but well dispersed on the surface [59]. The XRD pattern from titania particles exhibit broadened peaks which is due to finite size effect and can be described in terms of Scherrer formula [60]. The average crystallite size has been calculated from FWHM of the most prominent diffraction peak using Debye Scherrer equation

$$d = 0.91 * \lambda / \beta * \cos 2\Theta \qquad \ldots\ldots\ldots\ldots (1)$$

λ: wavelength of Cu-Kα , β:full width at half maxima, Θ: Bragg's angle

and found to be in the range of 7-8nm as shown in the table 1. From the table 1 it is concluded that with the increase in dopant concentration, the particle size decreases.

Table 1 shows the crystallite size of Al doped TiO_2 calcined at 500^0C

S.No.	Sample	%age of dopant	Calcination temperature	Crystallite size (nm)
1.	Doped TiO_2	0.1% Al_2Cl_3	500^0C	8.790
2.	Doped TiO_2	1% Al_2Cl_3	500^0C	8.199
3.	Doped TiO_2	5%Al_2Cl_3	500^0C	7.991

Table 1

Figure 4.3 shows the diffraction spectra of TiO_2 particles doped with 0.1, 1 and 5% aluminium calcined at 700^0C. The crystalline phase of the doped titania particles was identified to be anatase form as compared with JCPDS card no. 86-1156. Aforementioned, the particle size is calculated using scherrer formula is shown in table 2.

From the table 2 it is concluded that the particle size varies from 13-18nm. As compared to table 1 with increase in calcination temperature the crystallite size increases.

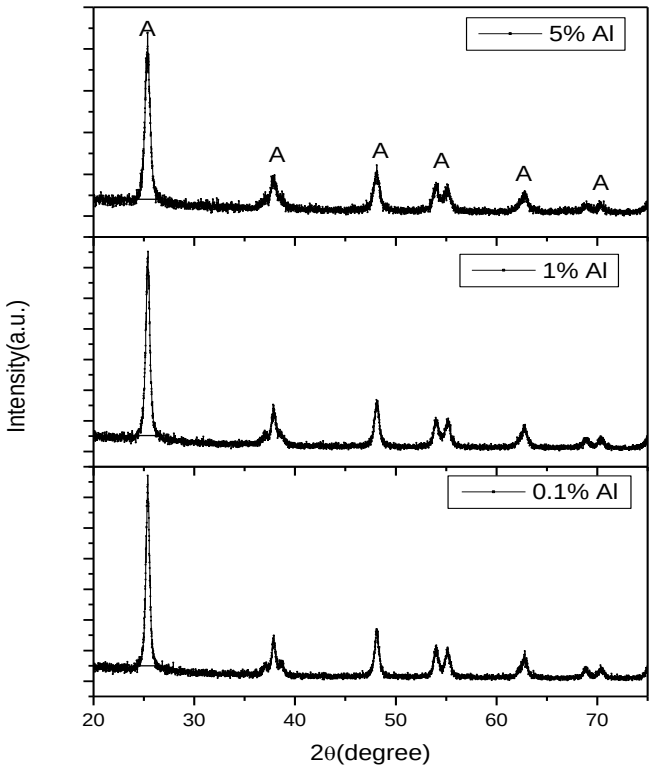

Figure 4.3 XRD pattern of TiO_2 doped with aluminium at 700^0C

Table 2 shows the crystallite size of Al doped TiO_2 calcined at 700^0C

S.No.	Sample	%age of dopant	Temperature of calcination	Crystallite size (nm)
1.	Doped TiO_2	0.1% Al_2Cl_3	700^0C	18.588
2.	Doped TiO_2	1% Al_2Cl_3	700^0C	15.490
3.	Doped TiO_2	5%Al_2Cl_3	700^0C	13.280

Table 2

Figure 4.4 shows the diffraction spectra of TiO_2 particles doped with 0.1,1 and 5% aluminium calcined at 900^0C. The crystalline phase of the doped titania particles was identified to be anatase and rutile form as compared with JCPDS card no.8,60,148. The particle size has been calculated using Scherrer formula and shown in table 3. From the

table 3 particle size varies from 39-51nm. With increase in calcination temperature the diffraction peak for the most dense plane get sharper indicating the increase in crsytallanity. The graphs show that the intensities of the anatase peaks decreased, while the intensities of the rutile peaks greatly increased and contents of rutile phase increased as the calcinations temperature was raised [61]. A phase transformation from anatase to rutile occurred for annealing temperatures at 900^0C and will be completed after 1200^0C [62].

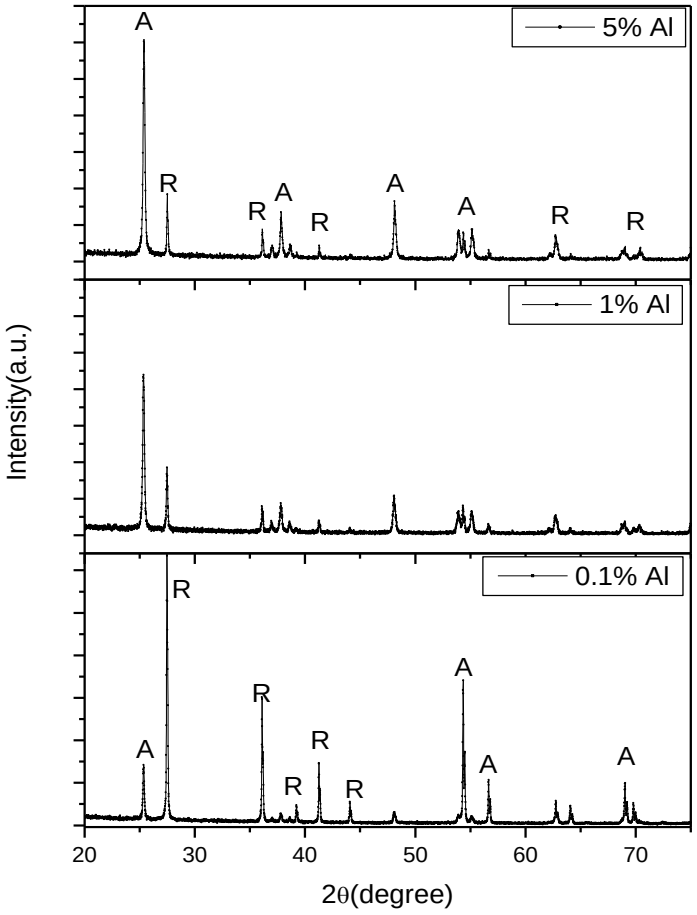

Figure 4.4 XRD spectra of TiO_2 doped with aluminium at 900^0C

Table 3 shows the crystallite size of Al doped TiO_2 calcined at 900^0C

S.No.	Sample	%age of dopant	Temperature of calcination	Crystallite size (nm)
1.	Doped TiO_2	0.1% Al_2Cl_3	900^0C	51.740

2.	Doped TiO_2	1% Al_2Cl_3	900^0C	39.830
3.	Doped TiO_2	5%Al_2Cl_3	900^0C	39.830

Table 3

4.2 Transmission Electron Microscopy:-

Sample for TEM were prepared by sonicating the TiO_2:Al powder in ethanol for 30 min, and a drop of the resulting suspension was placed on a copper grid [63]. TEM micrographs show the particles having size in the range of 7-9 nm. The particles are uniformly distributed and monodispersed having nearly spherical shape. The average particle size from TEM micrographs are well matched as calculated by Debye Scherrer eq. (1, 64).

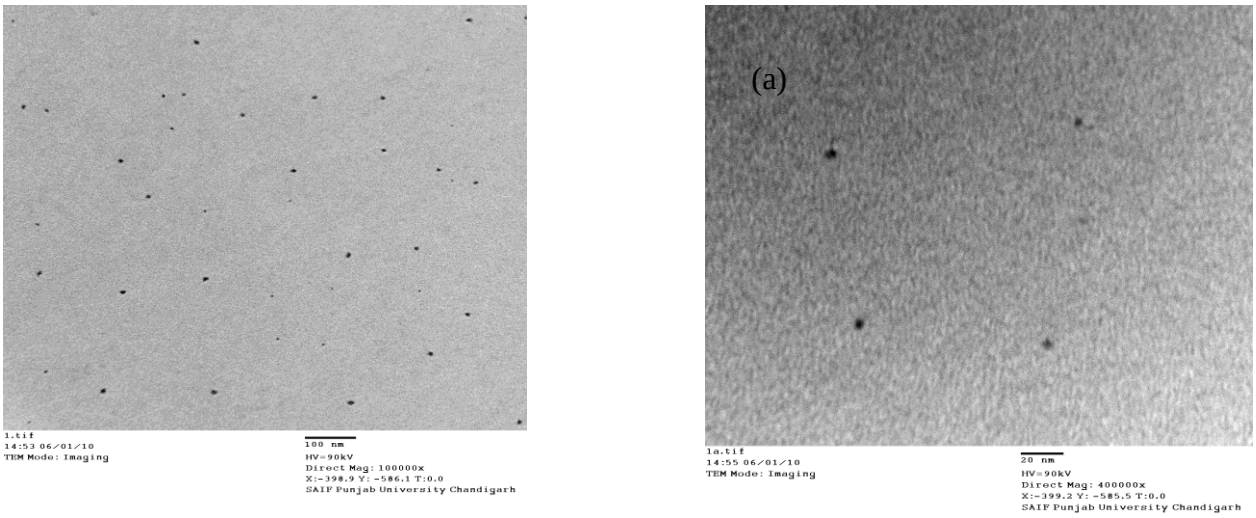

(a) (b)

Fig 4.5 The TEM images of 5%Al doped TiO_2 calcined at 500^0C

4.3 Scanning Electron Microscopy:-

Scanning electron microscope (SEM) was used for morphological study of TiO_2 :Al nanoparticles. SEM micrograph shows that the particles are nearly spherical. The individual spherical particles are not clearly observed due to the formation of nanoclusters during the growth [65].

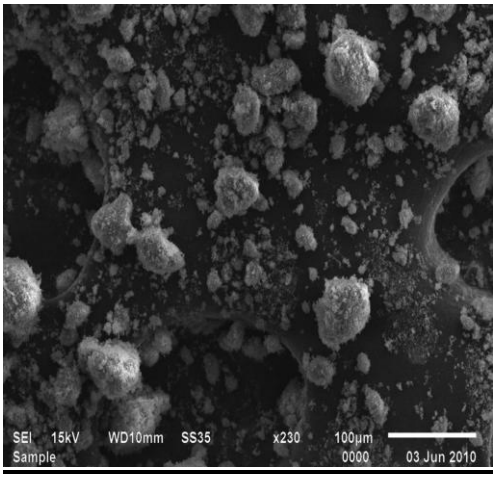

Fig 4.6 The SEM images of undoped TiO_2

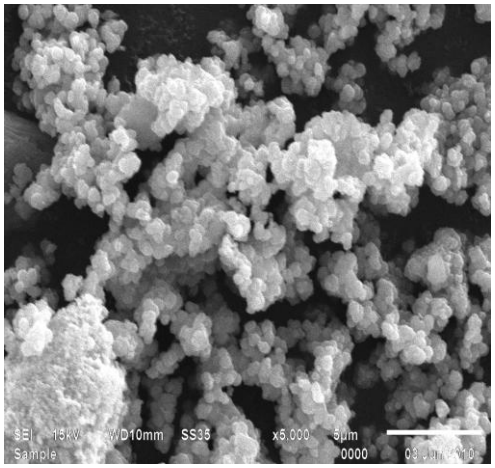

Fig 4.7 The SEM images of 1% Al doped TiO_2 calcined at 500^0C

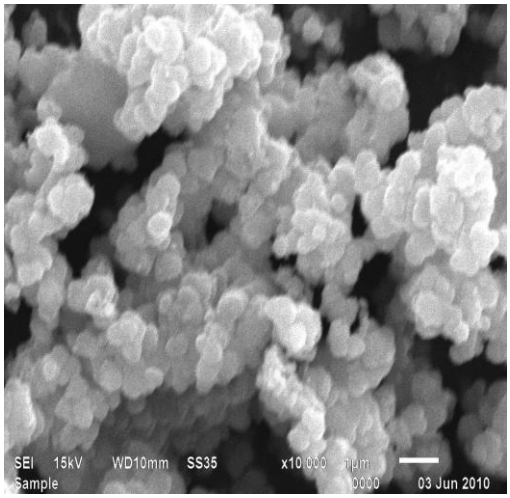

Fig 4.8 The SEM images of 5% Al doped TiO_2 at 500^0C

4.4 Energy dispersive X-ray spectroscopy:-

The elemental composition of TiO_2 doped with aluminium was analyzed by EDAX spectroscopy. Figure 4.9, 4.10 and 4.11 shows the EDAX spectra of TiO_2 doped with 0.1, 1 and 5% aluminium [66].

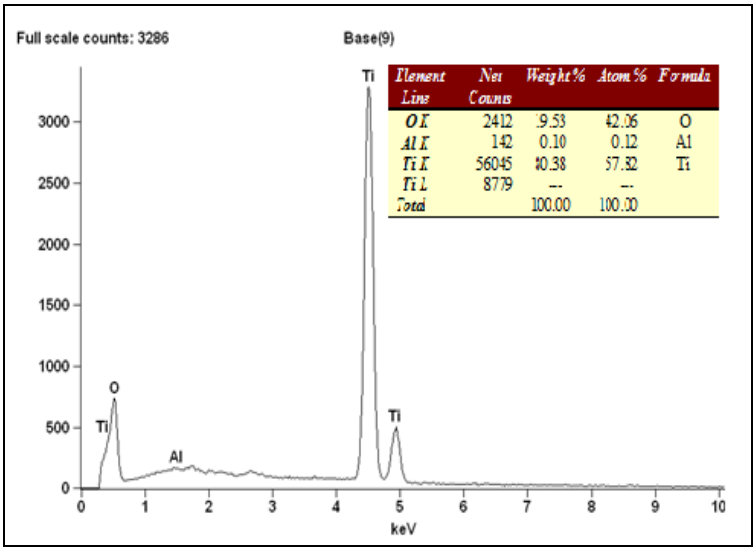

Figure 4.9 EDAX spectra of TiO_2 doped with 0.1% aluminium

From the figure 4.9 oxygen (in 0-1eV energy range), aluminium (in 1-2 eV energy range) and titania (in 4-5 eV energy range) has been observed. The atom % of Ti, Al and O is 57.32, 0.12 and 42.06 respectively.

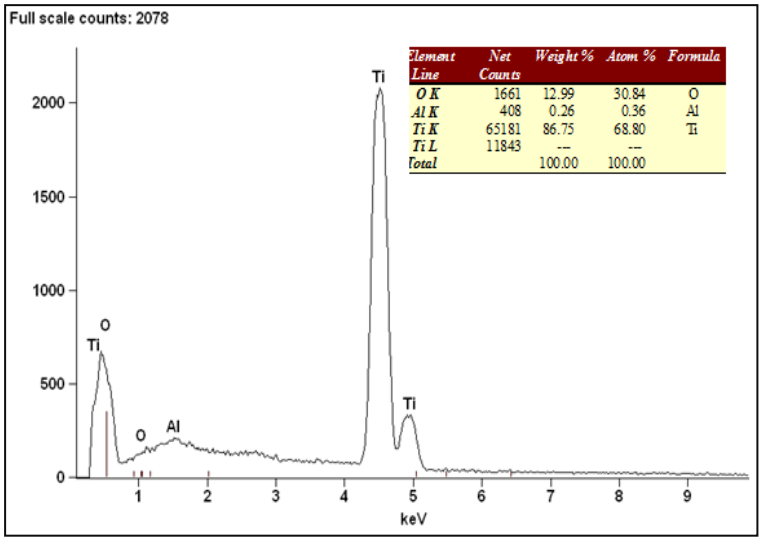

Figure 4.10 EDAX spectra of TiO_2 doped with 1% aluminium

From the figure 4.10 oxygen (in 0-1eV energy range), aluminium (in 1-2 eV energy range) and titania (in 4-5 eV energy range) has been observed. The atom % of Ti, Al and O is 68.80, 0.36 and 30.84 respectively.

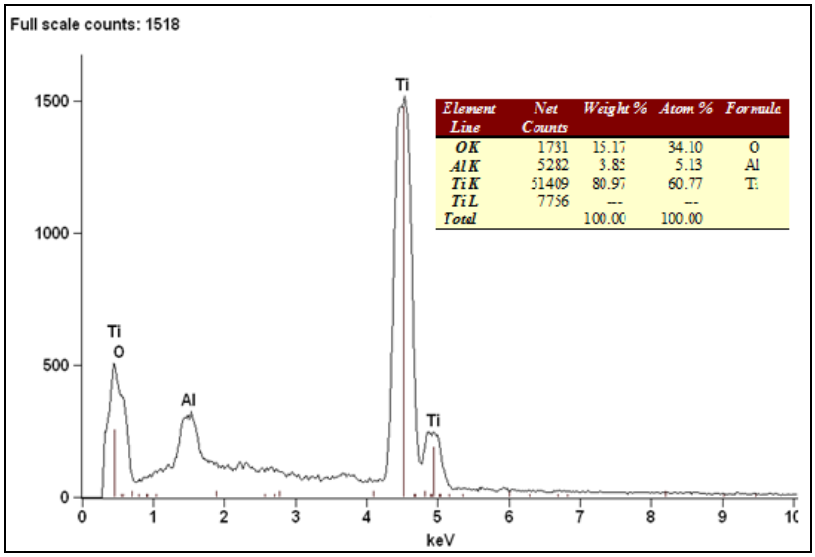

Figure 4.11 the EDAX spectra of TiO_2 doped with 5% aluminium

From the figure 4.11 oxygen (in 0-1eV energy range), aluminium (in 1-2 eV energy range) and titania (in 4-5 eV energy range) has been observed. The atom % of Ti, Al and O is 60.77, 5.13 and 34.10 respectively.

4.5 Photoluminescence Study

Figure 4.12 shows the emission spectra of titania nanoparticles. The excitation wavelength is set 370nm. Two emission peaks are observed at 430 nm and 473 nm respectively.

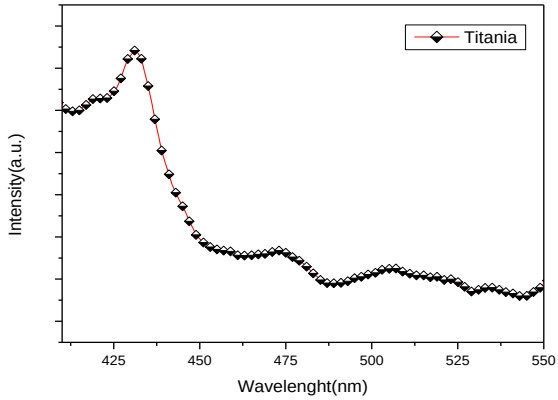

Figure 4.12 The emission spectra of the undoped titania

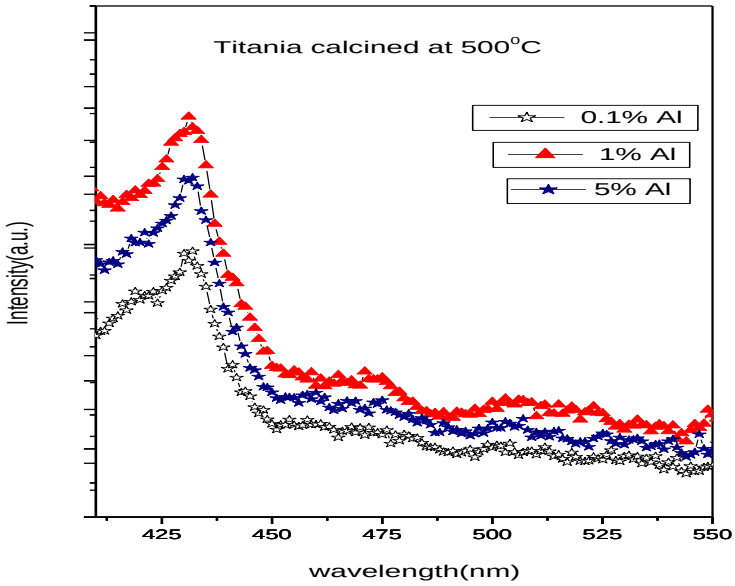

Fig 4.13 The emission spectra of TiO_2: Al at 500^0C

The available reports on the emission properties of semiconductor oxide nanomaterials, particularly for TiO_2, are not clear in the literature. The occurrence of emission peaks in the visible region is due to the presence of defect levels below the conduction band. The broad peak observed in the visible region is attributed to the electronic transition mediated by the defect levels such as oxygen vacancies in the band gap. In addition to these two major peaks observed in the PL spectrum, some vibrational levels are also seen in the fine structure [67].

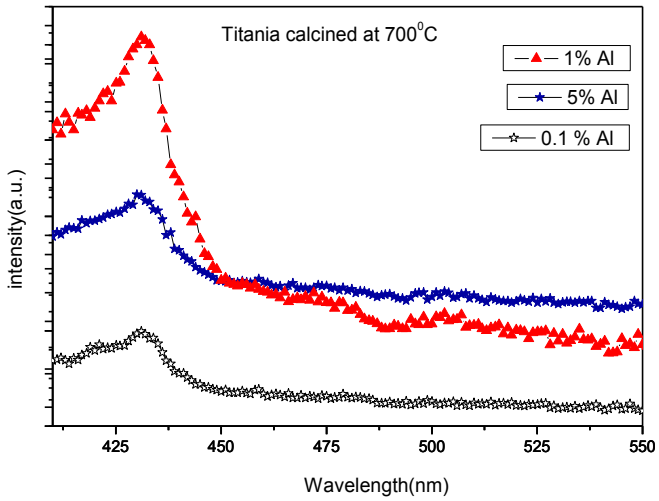

Fig.4.14 The emission spectra of TiO_2 : Al at 700^0C

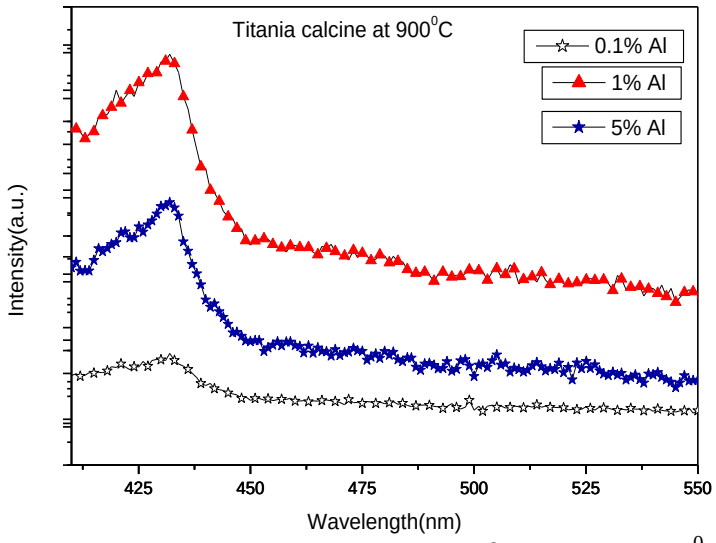

Figure 4.15 the emission spectra of TiO_2:Al at 900^0C

Figure 4.13, 4.14 and 4.15 shows the PL spectra of aluminium doped TiO_2 calcined at 500, 700 and 900^0C respectively. The results show that Al^{3+} did not enter into the crystal lattices of TiO_2 and was uniformly dispersed onto TiO_2, Al dopant did not give rise to a new PL signal, but it could improve the intensity of PL spectra with a appropriate Al content, which was possibly attributed to the increase in the content of surface oxygen vacancies and defects after doping Al [68].

4.6 UV-Visible spectroscopy:-

The optical absorption spectra of the nanocrystallites were recorded using UV-Vis spectrophotometer. The nanocrystallites powder has been suspended in ethanol and their optical absorption spectrum has been recorded at room temperature over the range 200 to 600 nm. Fig. 4.16 shows the absorption spectra of these samples.

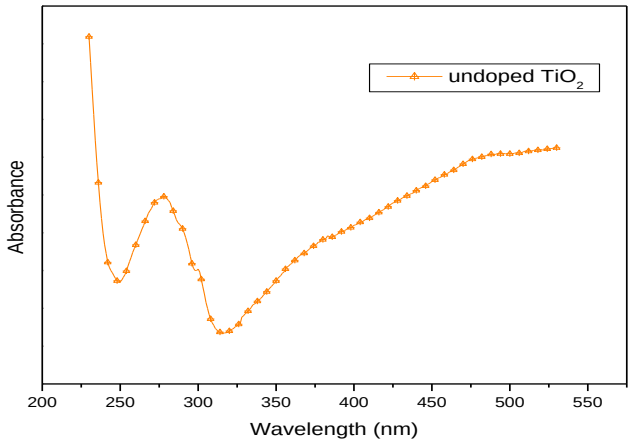

Fig. 4.16 UV-vis spectra of undoped TiO_2 nanoparticles

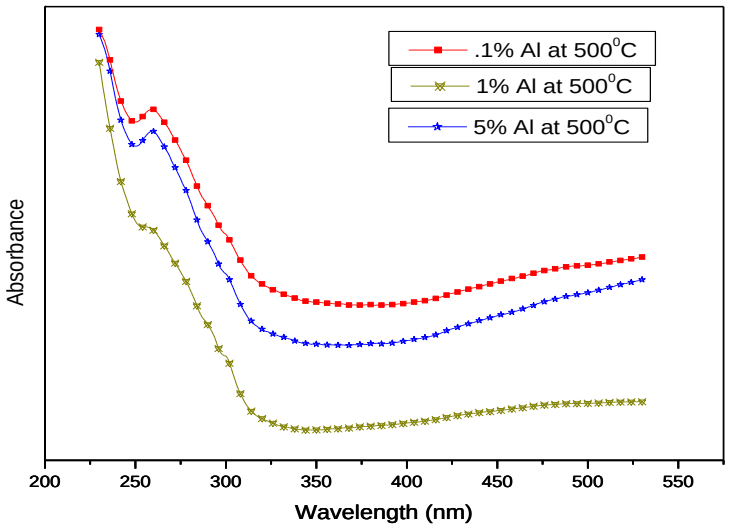

Fig.4.17 UV-Vis spectra of Al-doped TiO_2 nanoparticles calcined at 500^0C

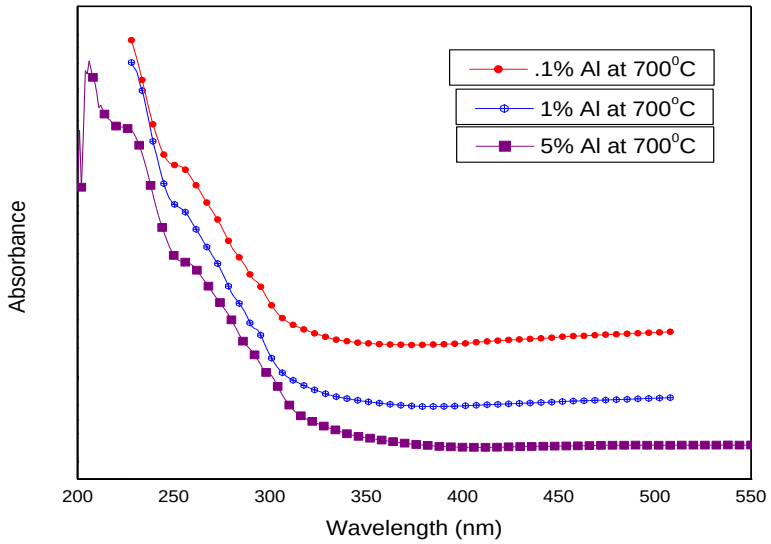

Fig.4.18 UV-Vis spectra of Al-doped TiO_2 nanoparticles calcined at 700^0C

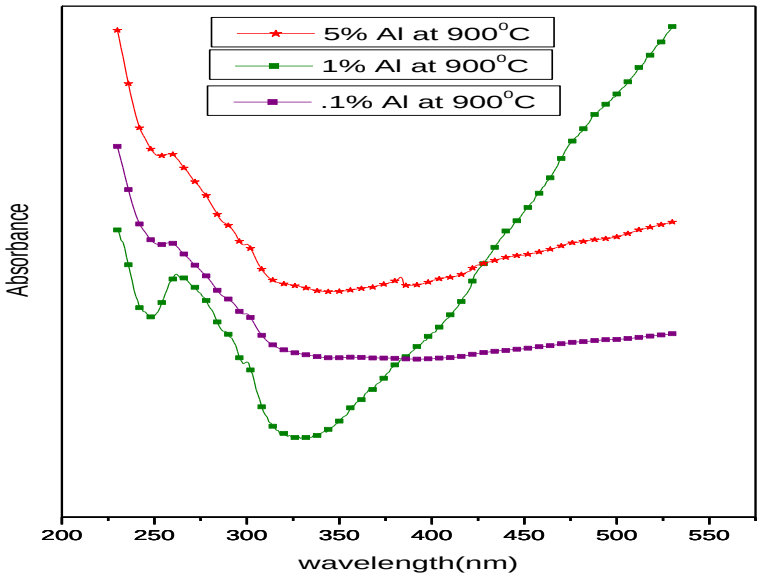

Fig.4.19 UV-Vis spectra of Al-doped TiO_2 nanoparticles calcined at 900^0C

.

It is clear from Fig. 4.16 that all the samples exhibit absorption edges. The absorption edges for different sized nanoparticles arise from quantum confinement effect. The broad absorption edge of the spectrum is the result of distribution of anatase nanoparticles at different size regime [69].

The fundamental absorption, which corresponds to electron excitation from the valence band to conduction band, can be used to determine the value of the optical band gap. The value of optical band gap is calculated by extrapolating the straight line portion of $(\alpha h\nu)^2$ vs hν graph to hν axis

Table 4 shows the band calculations:-

S.No.	Sample	Dopant concentration	Calcination tempreature	Band gap
1.	Undoped TiO_2	----------	---------	3.80eV
2.	Doped TiO_2	5 % Al	500^0C	4.21eV
3.	Doped TiO_2	1% Al	500^0C	4.18eV
4.	Doped TiO_2	0.1% Al	500^0C	4.15eV

5.	Doped TiO_2	5% Al	700^0C	4.00eV
6.	Doped TiO_2	1% Al	700^0C	3.95eV
7.	Doped TiO_2	0.1% Al	700^0C	3.90eV
8.	Doped TiO_2	5% Al	900^0C	3.80eV
9.	Doped TiO_2	1% Al	900^0C	3.78eV
10.	Doped TiO_2	0.1% Al	900^0C	3.72eV

Table 4

4.7 Reflectance Study

Figure 4.17 shows the diffuse reflectance spectra of TiO_2 nanoparticles doped with 5% aluminium calcined at different temperatures. The curves 4.17 (a), (b) and (c) show the diffuse reflectance spectra of doped samples calcined at 500^0C, 700^0C and 900^0C having diffuse reflectance 97-99%, 94-99% and 92-99% respectively for the visible region. The curve 4.17(d) shows the diffuse reflectance spectra of uncalcined undoped sample having diffuse reflectance 92-99%. With increases in the calcination temperature there is decreases in the reflectance, this might be due to lager particle size. With increases in calcination temperature there is increase in the size of grain boundary hence lager the particle size. From XRD it is well concluded that with increases in the calcination temperature there is increases in the crystallite size, so from the diffuse reflectance spectra it is well concluded that particle having smaller size show maximum reflectance [70]. For curves 4.17(a), (b) and (c) there are small kinks at 425, 560 and 580nm these might be due to defects and surface states. From the PL study it is found that the small kink at 425nm is due to O_2^{2-} vacancy and this is reported by many other researchers, similarly the kink the 560 and 580 can be assign defects and surface states that might be due O_2^{2-} vacancy of due to additional energy level introduced by Al. As the Al atoms are not incorporated into titania lattice, the luminescence peak is not obtain from the PL spectra. The curve 4.17(d) shows that there is a continuous decrease in the reflectance as one moves from 700 to 400nm region conforming the amorphous nature of titania.

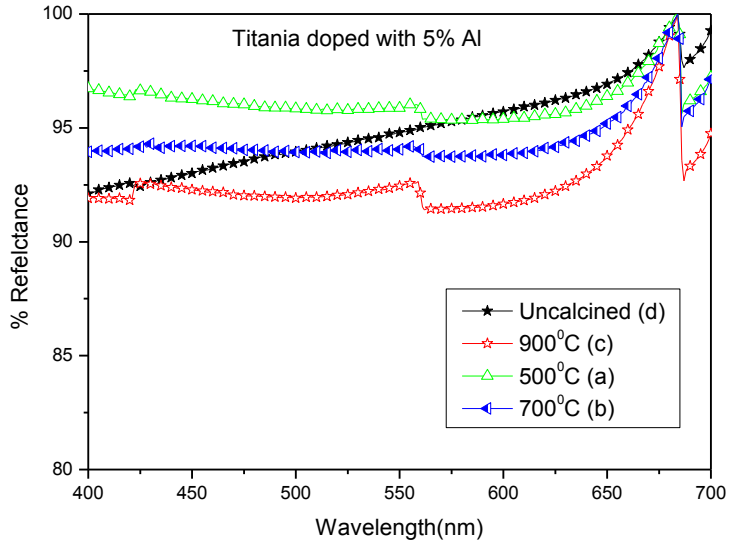

Figure 4.20 The diffuse reflectance spectra of TiO_2 calcined at different tempreatures

Chapter 5

Conclusions

5.1 Conclusions

Titania doped with different molar concentrations of Al have been synthesized using sol-gel technique. The effect of dopant concentration and calcination temperature on the particles diffuse reflectance has been studied.

After analyzing the results, following conclusions have been drawn.

- Anatase and rutile phase of titania at different calcination temperatures have been confirmed by XRD. No impurity peak was observed in the diffraction pattern excluding the probability of Al in the titania lattice. XRD pattern shows that crystallite size increases as the calcination temperature increases. With increase in calcination temperature, the diffraction peaks for the most dense plane get sharper indicating the increase in crsytallanity. Also crystallite size decreases as the molar concentration of dopant increases.

- Surface morphology of the NPs was studied by SEM and TEM. The NPs have been found to nearly spherical shape and possesses average size of ~ 7-9 nm.

- Using EDX, elemental analysis for TiO_2 doped with 0.1% Al has atomic % of Ti, Al and O respectively as 57.32, 0.12 and 42.06; and when TiO_2 is doped with 1% Al, atomic % of Ti, Al and O has been found to be respectively 68.80, 0.36 and 30.84; and when TiO_2 doped with 5% Al, it is respectively Ti, Al and O 60.77, 5.13 and 34.10.

- The optical band gap values for undoped and doped TiO_2 nanoparticles have been calculated using UV-Vis absorption spectra and are found to vary from 3.72 eV to 4.2 eV. It shows that band gap of TiO_2 increases as the molar concentration of dopant increases.

- The study of defects and color centre using photoluminescent spectra of doped and undoped TiO_2 nanocrystals, calcined at different temperatures, shows that all the plots contain two peaks centered at 430 and 470nm, and appearance of this peak is attributed to the presence of oxygen vacancies.

- The reflectance spectra of doped NPs calcined at 500^0C shows 97-99% reflectance as compared to uncalcined undoped NPs having 91-99% reflectance for the visible region.

Thus we conclude that TiO_2 nanoparticles doped with 5% Al calcined at 500^0C is found to be a potential material for reflective pigments, which find application in luminaries, search and spot lights, reflective panels, integrating spheres, photomultiplier tubes etc.

References:-

1. History of nanotechnology, Hyperlink; http://www.wikipedia.org
2. Dr. Wolfgang Luther Application of nanotechnology in energy sector
3. Nanotechnology, Hyperlink tionanostructure.wordpress.com/.../
4. Nanotechnology, Hyperlink; http://atomic-molecular-optical-physics
5. Nanoscale, Hyperlink; nanopedia.case.edu/NWPage.php?page=nanoscale
6. Jyoti S. A. Bhat Heralding a new future – Nanotechnology?
7. Dr. Wolfgang, Luther Application of nanotechnology in energy sector
8. Paul Holister, Jan- Willem Weener, Cristina Roman, Tim Harper, journal of nanopaticles.
9. Ogawa H, Nishikawa M and Abe A, Journal of Applied Physics(1982), vol 53 4448
10. Applications, Hyperlink, lib.bioinfo.pl/app/webroot/img/UserFiles/6594...
11. Reflectance,Hyperlink;wikipedia.org/wiki/Reflectivity
12. Reflectance, Hyperlink; greenisglobal.net/calculate-energy-savings-wi...
13. Reflectance, Hyperlink; journalofvision.org/3/5/3/article.aspx
14. Types of reflectance, Hperlink;micro.magnet.fsu.edu/.../specular/index.html
15. Specular reflection, Hyperlink; www.lightandmatter.com/html_books/5op/ch01/fi
16. Specular reflection image, Hyperlink; micro.magnet.fsu.edu/.../specular/index.html
17. Diffuse reflectance, Hyperlink;www.siggraph.org/education/.../diffuse_reflection.htm
18. Diffuse reflectance image, Hyperlink; www.screentekinc.com/glossary/glossary-def.shtml
19. Diffuse reflectance, Hyperlink;www.physicsclassroom.com/class/refln/u13l1d.cfm
20. Paints, Hyperlink; http://www.wikipedia.org/wiki/Paint
21. Oldendorf, William H. (2805 Angelo Dr., Los Angeles, CA, 90024)
22. Reflective paints, Hyperlink; http://www.isabeltilly.blogspot.com/
23. Pramod H.Borse et. al. J. of material sci. 13 (2002) p 553-559
24. Properties, Hyperlink; http://environmentalchemistry.com/yogi/periodic/Ti.html

25. Applications, Hyperlink; www.azom.com/Details.asp?ArticleID=1179
26. Rutile, Hyperlink; http://www.answers.com/topic/rutile
27. Anatase, Hyperlink; http://www.1911encyclopedia.org/Anatase
28. Yi Xie, Sung Hwan Heo, Yong Nam Kim, Seung Hwa Yoo and Sung Oh Cho
29. Applications, Hyperlink; www.azom.com/Details.asp?ArticleID=1179
30. Properties of aluminum, Hyperlink; http://www.azom.com/details.asp?ArticleID=1446
31. Scintag, Chapter-7 Basics of XRD (1999), Thermo ARL
32. B.D. Cullity, Elements of X-ray Diffraction (1979), Acta Crystallographica
33. Marta J.K. Flohr, X-Ray powder diffraction (1997), USGC
34. XRD, Hyperlink http://serc.carleton.edu/research_education/geochemsheets/techniques/XRD.html
35. S. Wischnitzer, Introduction to Electron Microscopy, (1981),BML QH 212 E4 W811i & TSB
36. J. Res. Natl. Inst. Stand. Technol.(2001), vol 106, 997–1012
37. Goodhew, Humphreys and Beanland, Electron Microscopy and Analysis 3 rd Edition, Taylor and Francis
38. EDX, Hyperlink; http://www.azonano.com/nanotechnology-quipment.asp?cat=52
39. Marco Cantoni, Chapter-13 introduction to Energy Dispersive X-ray
40. Kaufmann, Characterization of materials(2003), Willey interscience
41. D. Heiman, photoluminescence spectroscopy (2004)
42. Uses of pl , Hperlink, http://inventors.about.com/od/pstartinventions/a/Photoluminescen.htm
43. A. Borkowska, J. Domaradzki, D. Kaczmarek (2006),p-550-553
44. Yongfa Zhu, Li Zhang, Chong Gao and Lili Cao(2000), J. Mater. Sci., vol 35, p 4049-4054
45. G. Facchin, G. Carturan, R. Campostrini, S. Gialanella, L. Lutterotti, L. Armelao, G. Marcì, L. Palmisano and A. Sclafani(2000),J. Mater. Sci., vol 18, p 29-59
46. Borse, P. H.; Kankate, Laxman S.; Dassenoy, Fabrice; Vogel, Walter; Urban, Joachim; Kulkarni, Sulabha K.(2002), J. Mater. Sci. vol 13, p 553-559

47. S. Mayadevi, S. S. Kulkarni, A. J. Patil, M. H. Shinde, H. S. Potdar,S. B. Deshpande, S. K. Date(2000), J. Mater. Sci., vol 35, p 3943-3949
48. A. Vadivel Murugan, Violet Samuel and V. Ravi(2005), J. of Physics, vol 15, p 1-4
49. Xingzhao Ding, Lin Liu, Xueming Ma, Zhenzhong Qi, Yizhen He (1994), J. Mater. Sci., vol 13, p 462-464
50. Shaoyou Liu, Guocong Liu and Qingge Feng (2009), journal of porous material, vol 17, p 197-206
51. Sujith Perera and Edward G. Gillan, Chem. Commun.(2005), vol 5988, p 5988–5990
52. M.A. Behnajady ,N. Modirshahla M. Shokri B. Rad, Global NEST Journal (2008), vol 10, p 1-7
53. Q.R. Deng, Y. Gao, X.H. Xia, R.S. Chen, L. Wan, G. Shao, journal of physics(2009), vol 152, p 1-4
54. One day workshop on Fundamentals of Sol-Gel Technology September 1, 2007-ENSCM Montpellier-France
55. Sol-gel: a low temperature process for the materials of the new millenium by Jean Phalippou
56. Sol-gel method, Hyperlink; www.gitam.edu/.../bottamup%20app.htm
57. A. Wongkaow et al. Energy Research J (2010), vol 1, p73-77
58. Y. Bessekhouad et al. International J. of Photoenergy (2003), vol 5, p 153-158
59. G. Glaspell et al., J. Cluster Sci. Vol 16 dec(2005)
60. L. Mingee et al., Front Chem. China(2007), vol 2, p 278-282
61. Q. Xiao et al., Mater. Sci. and Engineering B(2007), vol 137 p 189-194
62. X. Ding et al., J. of Mater. Sci. Letters(1994), vol 13, p 278-282
63. Jing Tang et al., Nano Letters (2005), vol 5, p 543-548
64. Yong Zhou and Markers Antonuutti, J. AM. CHEM. SOC. (2003), vol 125, p 14960-14961
65. P.Dennis Christy et al., Cryst. Res. Technology (2009),vol. 44 , p 484-488
66. A. Wongkaow et al., Energy Research J (2010), vol 1, p 73-77
67. P.Dennis Christy et al., Cryst. Res. Technology (2009), vol. 44, p 484-488

68. J. Liqiang et al., J. of Solid State Chemistry (2004), vol. 177, p 3375-3382
69. F. H. Batal, Indian J. of pure and appl. Phy.(2009), vol 47, p 631-642
70. M. M. Mikhailov et al., Russian physics journal(1998), vol 41, p 1222-1228